

# A novel Digital Beam-Forming Concept for spaceborne Reflector SAR Systems

Sigurd Huber <sup>#1</sup>, Marwan Younis <sup>#2</sup>, Anton Patyuchenko <sup>#3</sup>, Gerhard Krieger <sup>#4</sup>

<sup>#</sup>*Institut für Hochfrequenztechnik und Radarsysteme, Deutsches Zentrum für Luft- und Raumfahrt e.V. (DLR)  
Münchener Straße 20, D-82234 Weßling*

<sup>1</sup>sigurd.huber@dlr.de

<sup>2</sup>marwan.younis@dlr.de

<sup>3</sup>anton.patyuchenko@dlr.de

<sup>4</sup>gerhard.krieger@dlr.de

**Abstract**—The trend in the conception of future spaceborne radar remote sensing is towards the use of digital beam-forming techniques. These systems will comprise multiple digital channels, where the analog-to-digital converter is moved closer to the antenna. This dispenses the need for analog beam steering and by this the use of transmit/receive modules for phase and amplitude control. Digital beam-forming will enable Synthetic Aperture Radar (SAR) which overcomes the coverage and resolution limitations applicable to state-of-the-art systems. Moreover, new antenna architectures, such as reflectors, already implemented in communication satellites, are being reconsidered for SAR applications. This paper introduces a new digital beam-forming radar concept based on the combination of a reflector with a digital feed array. For a system example the SAR performance is estimated. Finally a novel digital signal processing approach, exploiting the signal properties of the transmitted waveform, is presented.

## I. INTRODUCTION

Synthetic aperture radar, utilizing digital beam-forming, is increasingly being considered for future earth observation missions. This is evident both from research activities [1], [2] and space qualified technology demonstrations [3]. One of the reasons for this trend is that state-of-the-art SAR systems can not fulfill the heterogeneous demand on products at the required performance level. The motivation for using Digital Beam-Forming (DBF) techniques is their ability to provide simultaneously a wide swath (coverage) and a high resolution. In this paper, systems utilizing the various forms of DBF, such as SCan-On-REceive (SCORE), Conjugate Field Matching (CFM), etc. are jointly referred to as SMART, which stands for Smart Multi-Aperture Radar Techniques. In the most general sense, SMART sensors allow a relaxation of the system design parameters, by increasing the degrees of freedom. Specifically, for a given geometric resolution this results in systems with higher Signal-to-Noise Ratio (*SNR*) and lower ambiguity-to-signal ratio, both being key requirements on SAR systems. Equipped with digital receive channels, SMART sensors do not require analog phase and amplitude control of the received signals (analog beam-forming), yielding a receiver RF hardware free of transmit/receive modules. Complex control and calibration units can be realized with less hardware effort. Instead, SMART will push the development of onboard digital

signal processing capable of handling multiple channels of high data rate.

The sensor architecture considered here is a parabolic reflector in combination with a digital feed array consisting of multiple transmit/receive elements in elevation. Reflector antennas offer some unique advantages over conventional planar phased array systems. Unfoldable reflectors allow at relatively light weight a large aperture relaxing the power demands. Concerning the radiation characteristics it is possible to direct electromagnetic energy within a sharp beam, which minimizes losses at the swath borders in the transmit case.

## II. SYSTEM OPERATION: DIGITAL BEAM-FORMING IN ELEVATION

In 1981 Blythe [4] suggested a basic approach for analog beam-steering such that the receive beam moves over the swath in accordance with the direction of reflection. About twenty years later, his idea finds a more detailed description and justification in the independent and almost contemporaneous works by Kare [5], and Suess & Wiesbeck [6].

The patent by Kare in [5] presents the Moving Receive Beam as a technique to improve the quality of “high resolution SAR imagery over a wide target area”, by reducing the edge losses and the range ambiguities. Different approaches for the steering of the receiving beam are suggested: based on an a priori assumption on the acquisition geometry, openloop system; on the actual receive data, closeloop system; or on test pulses. Moreover, Kare describes different analog feed implementation options, involving both planar array and reflector architectures, showing a thorough understanding of the implications in the reflector case. The necessity to take into account the temporal extension of the pulse in the steering mechanism is mentioned, and in particular for chirp pulses, the possibility to adapt the position of the beam to the frequency of the received signal.

In [6] and [7] for the first time digital beam-forming techniques are presented in conjunction with a time varying receive beam-steering in elevation. A quantitative description of the steering law, consisting of a compensation for the time spread of chirp pulses by using a frequency dependent steering is given.

### III. REFLECTOR SYSTEM ARCHITECTURE

The reflector system consists of a parabolic reflector and a feed array of transmit/receive elements, as shown in Fig. 1. The feed elements are arranged in the plane perpendicular to the flight direction and facing the reflector. Each element results in a beam, illuminating a region on the ground, which partially overlaps with the region illuminated by the beams of the adjacent elements. To illuminate a given angular segment in elevation, the corresponding feed elements are activated. Depending on the scan angle, one or more elements need to be activated, to avoid *SNR* loss. The receive beam will scan the complete swath within the time period of one *PRI*, whereas each element is only active during a subinterval of this time period. On transmit all  $N$  elements are activated generating a wide beam.

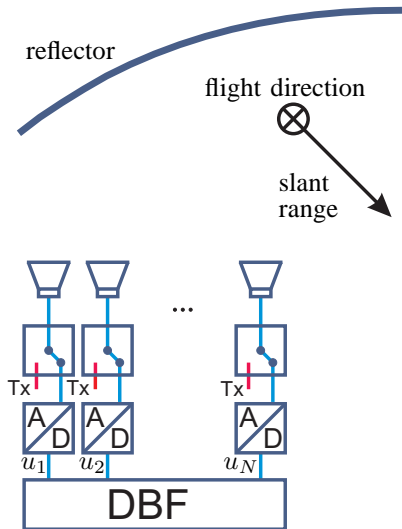


Fig. 1. System architecture for reflector system; some components such as LNAs, T/R-modules, mixers, filters etc. are not shown to maintain a clear representation.

### IV. REFLECTOR SYSTEM DESIGN

In order to give reasonable performance predictions, a design example based on the parameters listed in Tab. I is derived. To cover the complete swath a half power beam width

TABLE I  
PERFORMANCE PARAMETERS

Parameter		Value
frequency	C-Band	5.4 GHz
swath width		$\geq 120$ km
resolution (range, azimuth)	$\delta_{rg}, \delta_{az}$	$\leq 8 \times 8$ m
ambiguity-to-signal ratio	<i>RASR, AASR</i>	-20 dB
noise-equivalent sigma zero	<i>NESZ</i>	-25 dB

of  $7.3^\circ$  in elevation is required. The beam width in azimuth is primarily determined by the azimuth resolution and calculated to  $0.2^\circ$ . The degrees of freedom for the design are the focal length, the diameter, and the feed array geometry [8]. The schematic design of the reflector antenna with feed array is

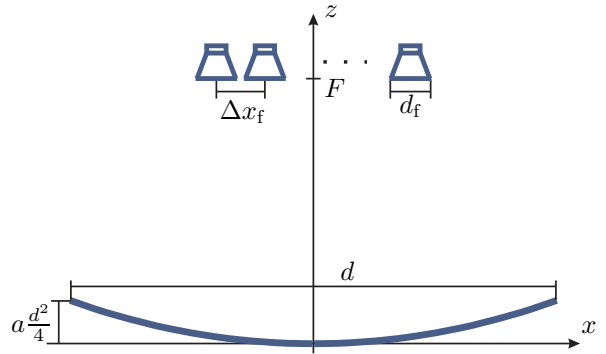


Fig. 2. C-Band reflector and feed array geometry.

presented in Fig. 2. The feed array is positioned symmetrically in front of the reflector in the focal plane  $z = F$ , neglecting the effect of blockage. Here the elevation plane is defined in the Cartesian reflector coordinate system with  $y = 0$ , with the azimuth direction orthogonal to this plane. The diameter  $d$  of the reflector is 10 m. With a focal length  $F$  of 5.7 m, the shape parameter  $a$ , which defines the  $z$ -coordinate of each surface point of the paraboloid, can be determined as  $a = 1/(4F)$ .

The feed array is a linear array consisting of 26 elements, facing the plane  $z = F$ . This allows beam steering in elevation direction. The spacing  $\Delta x_f$  of adjacent elements is  $0.58\lambda$ . For quadratic  $0.4\lambda$  patches, the dimensions of the (passive) patch array, allowing for sufficient margin, is approximately  $85 \text{ cm} \times 5 \text{ cm}$ .

### V. DIGITAL BEAM-FORMING CONCEPTS

Generally the digital beam-forming concepts, considered in this paper, aim at an improvement of the system performance, namely the signal to noise ratio (*SNR*) as well as the robustness of the phase against pointing errors.

The input to the digital beam-former is an  $N$ -dimensional raw data vector  $\mathbf{u}^T(t) = [u_1 u_2 \dots u_N]^T(t)$  as indicated in Fig. 1. This signal is modeled as the transmitted waveform  $s(t)$  weighted with the individual complex channel pattern  $\mathbf{g}^T(\theta) = [g_1 g_2 \dots g_N]^T(\theta)$  and superimposed by thermal receiver noise  $\mathbf{n}^T(t) = [n_1 n_2 \dots n_N]^T(t)$  of power proportional to the receiver bandwidth.

$$\mathbf{u}(t) = \mathbf{g}(\theta)s(t) + \mathbf{n}(t) \quad . \quad (1)$$

The sampled beam-former output is a weighted linear combination of the input raw data signals

$$u_{\text{DBF}}(k) = \mathbf{w}^T(k)\mathbf{u}(k) \quad . \quad (2)$$

Based upon this equation different digital beam-forming techniques are introduced in the next subsections.

#### A. Scan on Receive

The SCan-On-Receive (SCORE) mode of operation is primarily based on generating a wide transmit beam that illuminates the complete swath and a narrow, high gain beam on receive that follows the pulse echo on the ground. Adverse to planar phased array antennas, in the reflector case a single

activated feed element allows to illuminate only a small solid angle. This means that adjacent feed element patterns do not overlap substantially. The consequence is that during the scan process different receive channels have to be switched on or off. The number of activated elements at a given time instance is dictated by the duration of the pulse. Looking at a certain

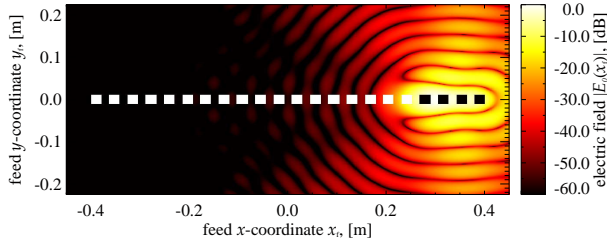


Fig. 3. Normalized electric field on the feed array due to an extended pulse on the swath edge.

direction  $\theta$ , the corresponding channel has to be open until the signal completely has entered the system. The longer the pulse the longer the channel has to be activated. Since the echo on ground moves on, additional receive elements have to be switched on. Fig. 3 shows the field strength distribution on the feed plane due to an extended pulse in near range, corresponding to an angular extent of  $0.86^\circ$ . The field is concentrated over a subset of feed elements, where the activated elements are represented by black patches.

In the notation of equation (2) the corresponding weight vector would look like this:

$$\mathbf{w}^\top(k) = [0\dots 01111]^\top, \quad (3)$$

where 1 denotes an activated feed element and 0 indicates a switched off channel. By this rudimentary beam-forming method it becomes clear, that the receive gain will drop proportional to the number of activated elements. Nevertheless for this design and duty-cycles  $dc \sim 8\%$  the optimum selection of activated channels is four.

### B. Conjugate Field Matching

To overcome the large gain loss, a time varying weighting method, based on the Conjugate Field Matching (CFM) [9] principle can be applied. By this method the individual channel weights are chosen as the conjugate complex of the incident field on the feed elements.

$$\mathbf{w}(k) = \frac{\mathbf{g}^*(k)}{\mathbf{g}^\top(k)\mathbf{g}^*(k)}. \quad (4)$$

In principle CFM allows to activate all  $N$  channels on receive simultaneously. Those channels contributing predominantly with noise are quasi nulled with small magnitude weights. Since the signals are also combined according to their phase, the high receive gain can be reconstructed at every time instance.

### C. Frequency Adaptive Filtering

The afore mentioned principles are adequate for short pulse lengths. Consider the baseband raw data signal  $u_i$  in Fig. 4(a) originating from two point scatterers. The selected waveform is a chirp, common for spaceborne SAR. Since both scatterers are observed under different aspect angles, they are also weighted with different feed element patterns. Consequently the weight

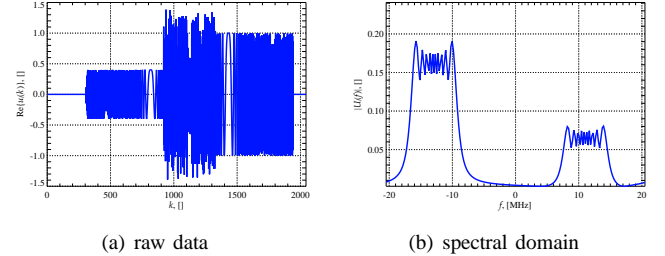


Fig. 4. Raw data signal  $u_i$  for two point scatterers for a single channel (left); Fourier spectrum of the raw data stream sequence (right)

$w_i$  chosen for example for  $k = 1000$  can only match the one signal or the other. The solution to this problem is the use of a frequency adaptive filter. Taking the Fourier transform of the overlap region between  $k = 1000$  and  $k = 1200$  results in two separated spectra. In Fig. 4(b) the low frequency part of the large amplitude signal can be clearly distinguished from the high frequency part of the low amplitude signal. Each spectral part can now be weighted individually. The filter can be implemented as a finite impulse response filter (FIR). This digital beam-forming approach overcomes the limitations from temporally extended pulses.

### D. Simulation Results

In the following, simulation results for four different digital beam forming algorithms are presented. The first algorithm serves as a reference, since it is independent from the pulse length and therefore performs optimal. The basic idea is to range compress the individual channel raw data streams prior to beam forming. The raw data signals of the activated channels  $N_{\text{act}}$  are then combined utilizing CFM according to equation (4). The draw back is clearly the high standard of the digital beam former hardware, where digital filters with thousands of coefficients would be required. The second algorithm is the frequency adaptive beam former. Here raw data blocks of 256 samples are processed individually for the selected channels. Obviously the hardware requirements are relaxed, since only FIRs with 256 coefficients are necessary. The raw signals are then again combined via CFM. The last two algorithms are the basic unity weighting beam former (3) and the CFM algorithm (4), without any further processing.

Fig. 5 shows a realization of the relative  $SNR$ . Here a backscatter, modeled by a stationary circular complex Gaussian process, is assumed. Clearly the frequency adaptive beam former (blue curve) outperforms the unity weighting approach (green curve) by 1.5 dB. Also CFM without further processing (red curve) suffers from non ideal weighting. Looking at

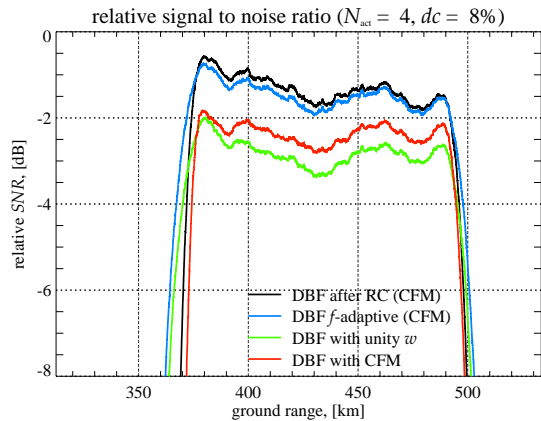


Fig. 5. Normalized  $SNR$  for 4 activated channels and 8% duty cycle.

the pointing induced phase error in Fig. 6, the advantage of frequency adaptive filtering becomes even more evident. For

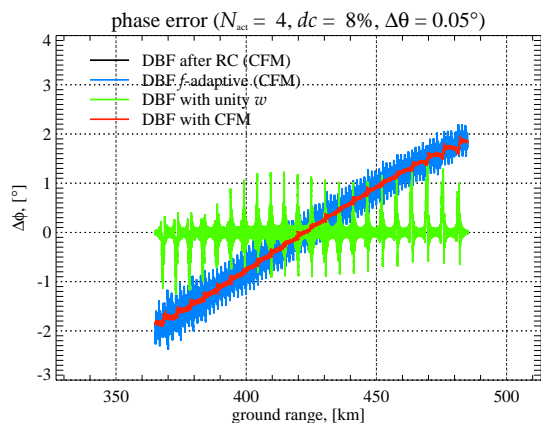


Fig. 6. Mispointing induced phase error simulation without thermal receiver noise.

a mispointing  $\Delta\theta$  of  $0.05^\circ$ , the CFM based DBF approaches result in a nearly linear phase ramp, while the unity weighting algorithm produces periodic phase jumps, which cannot be calibrated. The frequency adaptive beamformer phase error is more noisy due to the blockwise processing.

## VI. CONCLUSION

This paper presents an innovative antenna architecture that employs the technique of digital beam-forming on receive to improve the imaging performance and radiometric resolution of future SAR systems without losing wide swath coverage. As an alternative to a planar antenna, the novel idea to combine a reflector antenna with a digital feed array to enhance the performance of future SAR systems was introduced. Unfoldable reflector antennas have a high potential to significantly increase the receiving aperture and by this both the range ambiguity suppression and the  $NESZ$  if compared to planar arrays where the size of the antenna is usually restricted by the limited space in the launcher fairing.

Long chirp signals and large reflectors, however, require more sophisticated signal processing techniques to optimize the performance. A gain loss from long chirps can be avoided by frequency adaptive filtering. In consequence, one can take full advantage of the large apertures provided by present and future deployable reflector antennas. Reflectors with digital feed arrays are therefore a promising concept for future SAR systems with high potential to outperform planar arrays with regard to the SAR imaging performance for a given weight, size and cost budget.

## REFERENCES

- [1] G. Krieger, N. Gebert, and A. Moreira, "Multidimensional Waveform Encoding: A New Digital Beamforming Technique for Synthetic Aperture Radar Remote Sensing," *IEEE Transactions on Geoscience and Remote Sensing*, vol. 46, no. 1, pp. 31–46, Jan 2008.
- [2] G. Krieger, N. Gebert, M. Younis, F. Bordon, A. Patyuchenko, and A. Moreira, "Advanced Concepts for Ultra-Wide-Swath SAR Imaging," in *European Conference on Synthetic Aperture Radar (EUSAR)*, vol. 2, Jun 2008, pp. 31–34.
- [3] C. Fischer, C. Schaefer, and C. Heer, "Technology Development for the HRWS (High Resolution Wide Swath) SAR," in *International Radar Symposium (IRS)*, Sep 2007.
- [4] J. H. Blythe, "Radar systems," U.S. Patent 4,253,098, Feb, 1981.
- [5] J. T. Kare, "Moving receive beam method and apparatus for synthetic aperture radar," U.S. Patent US 6,175,326 B1, Jan, 2001.
- [6] M. Suess and W. Wiesbeck, "Side-looking Synthetic Aperture Radar System," European Patent EP 1 241 487 B1, Sep, 2002.
- [7] M. Suess, B. Grafmüller, and R. Zahn, "A novel high resolution, wide swath SAR," in *IEEE International Geoscience and Remote Sensing Symposium (IGARSS)*, vol. 3, 2001, pp. 1013–1015.
- [8] C. A. Balanis, *Antenna Theory: Analysis and Design*. John Wiley & Sons, Inc., 1997.
- [9] P. T. Lam, S.-W. Lee, D. C. D. Chang, and K. Lang, "Directivity Optimization of a Reflector Antenna with Cluster Feeds: A Closed-Form Solution," *IEEE Transactions on Antennas and Propagation*, vol. 33, no. 11, pp. 1163–1174, Nov 1985.